Air Quality, Atmosphere & Health (2022) 15:1507–1521
https://doi.org/10.1007/s11869-022-01178-z

Spatiotemporal variations and sources of $PM_{2.5}$ in the Central Plains Urban Agglomeration, China

Xiaoyong Liu[1,2] · Chengmei Zhao[1,2] · Xinzhi Shen[3] · Tao Jin[3]

Received: 10 September 2021 / Accepted: 2 March 2022 / Published online: 6 July 2022

Abstract

The Central Plains Urban Agglomeration (CPUA) is the largest region in central China and suffers from serious air pollution. To reveal the spatiotemporal variations and the sources of fine particulate matter ($PM_{2.5}$, with an aerodynamic diameter of smaller than 2.5 μm) concentrations of CPUA, multiple and transdisciplinary methods were used to analyse the collected millions of $PM_{2.5}$ concentration data. The results showed that during 2017 ~ 2020, the yearly mean concentrations of $PM_{2.5}$ for CPUA were 68.3, 61.5, 58.7, and 51.5 μg/m^3, respectively. The empirical orthogonal function (EOF) analysis suggested that high $PM_{2.5}$ pollution mainly occurred in winter (100.8 μg/m^3, 4-year average). The diurnal change in $PM_{2.5}$ concentrations varied slightly over the season. The centroid of the $PM_{2.5}$ concentration moved towards the west over time. The spatial autocorrelation analysis indicated that $PM_{2.5}$ concentrations exhibited a positive spatial autocorrelation in CPUA. The most polluted cities distributed in the northern CPUA (Handan was the centre) formed a high-high agglomeration, and the cities located in the southern CPUA (Xinyang was the centre) formed a low-low agglomeration. The backward trajectory model and potential source contribution function were employed to discuss the regional transportation of $PM_{2.5}$. The results demonstrated that internal-region and cross-regional transport of anthropogenic emissions were all important to $PM_{2.5}$ pollution of CPUA. Our study suggests that joint efforts across cities and regions are necessary.

Keywords Central Plains Urban Agglomeration · $PM_{2.5}$ · Spatiotemporal variations · Potential sources

Introduction

Over the past decades, China has witnessed rapid economic development, industrial expansion, and urbanization, which have led to serious air pollution (Huang et al. 2014). Regional air pollution caused by fine particulate matter ($PM_{2.5}$, with an aerodynamic diameter smaller than 2.5 μm) occurs frequently in several key regions of China, e.g. Beijing-Tianjin-Hebei (BTH) (Gao et al. 2018; Ding et al. 2019), Yangtze River Delta (YRD) (Ming et al. 2017), Sichuan Basin (Tian et al. 2019), and Fenwei Plain (Zhai et al. 2019; Cao and Cui, 2021). A high level of $PM_{2.5}$ damages human health, impacts regional climate changes, and affects agricultural ecosystems (Feng et al. 2018; Cohen et al. 2017; Zhou et al. 2018). Frequent haze and increasing $PM_{2.5}$ concentrations have affected sustainable socioeconomic development, which draws public anxiety and extensive concerns. To address this difficult problem, many studies have been conducted by scientists to understand the levels, distribution, and sources of regional pollution (Liang et al. 2019; Ye et al. 2018). In response to extremely severe and persistent haze pollution, many government-backed measures have been taken to reduce haze events and improve air quality.

Recently, extensive studies have mostly focused on metropolises and regions in northern China, such as Beijing, Tianjin, Shijiazhuang, and BTH, to clarify the spatial and temporal

✉ Xiaoyong Liu
xyliu_liuxy@163.com

Chengmei Zhao
zhaocm@xynu.edu.cn

Xinzhi Shen
shenxinzhi6719@163.com

Tao Jin
jintao332005@163.com

[1] School of Geographic Sciences, Xinyang Normal University, Xinyang, China

[2] Henan Key Laboratory for Synergistic Prevention of Water and Soil Environmental Pollution, Xinyang Normal University, Xinyang, China

[3] Xinyang Ecological Environment Monitoring Centre, Xinyang, China

distribution of $PM_{2.5}$ (Xu et al., Xu and Zhang, 2020; Yan et al. 2018). Thus, only a few studies have focused on the Central Plains Urban Agglomeration (CPUA) region, which is an important growth pole of China's economy and is burdened by serious air pollution problems (Fu et al. 2020). As the largest urban agglomeration in Central China, CPUA includes 30 prefecture-level cities, namely all 18 cities in Henan Province, Changzhi, Jincheng, and Yuncheng in Shanxi Province; Liaocheng and Heze in Shandong Province; Huaibei, Bengbu, Suzhou, Fuyang, and Bozhou in Anhui Province; and Xingtai and Handan in Hebei Province (Liu et al. 2019; Fu et al. 2020). According to previous studies, Zhengzhou (the capital city of Henan Province), Jiaozuo, Pingdingshan, Xinxiang, and Anyang in Henan Province were all heavily polluted by $PM_{2.5}$, especially in autumn and winter (Feng et al. 2018; Jiang et al. 2018; Liu et al. 2021; Wang et al. 2021; Su et al. 2021). Xingtai and Handan in Hebei Province are two typical industrial cities with massive anthropogenic emissions and high $PM_{2.5}$ concentrations (Yang et al. 2018; Liu et al. 2020). Yuncheng in Shanxi Province is an intensive energy-consuming city and frequently experiences haze. Fu et al. (2020) reported that in CPUA, the health effect damage of $PM_{2.5}$ pollution was 11.1 million, and the health effect economic loss was 94.5 billion RMB in 2017. However, studies on the spatiotemporal variations in $PM_{2.5}$ from the perspective of CPUA are rare. Since 2013, the Chinese government has made a firm decision to reduce the $PM_{2.5}$ concentration and taken some measures to address air pollution (Chen et al. 2019; Jiang et al. 2020). Under such circumstances, the $PM_{2.5}$ concentration in CPUA has varied in recent years. Therefore, it is urgent to conduct relevant research to understand the $PM_{2.5}$ characteristics and sources in CPUA.

The present study aims to investigate the spatial and temporal variations and the potential geographical source of $PM_{2.5}$ in CPUA. Multiple transdisciplinary methods, including classical statistics, geographical analysis, spatial statistics, and potential source analysis, are employed in this study. Specifically, we (1) systematically demonstrate annual, seasonal, monthly, and diurnal variations in $PM_{2.5}$, (2) reveal the spatial distribution and variation, and (3) identify the potential geographical source regions and regional transport of $PM_{2.5}$.

Materials and methods

Study area and data sources

The CPUA (31.4° N ~ 37.8° N, 110.2° E ~ 118.2° E) is located in central and eastern China (Fig. 1a), including 30 cities (Fig. 1c). It covers 287,000 km^2 with a population of more than 160 million. CPUA is seriously constrained by resources and population agglomeration caused by its rapid urbanization that continues to pressure the ecological environment in this area and causes high aerosol loading (Shen et al. 2019).

A total of approximately 4.3 million data points were collected from January 1, 2017, to December 31, 2020. The pandemic of coronavirus disease 2019 (COVID-19) resulted in a stringent lockdown in China to reduce the infection rate. The distinct decrease in anthropogenic source emissions led to an improvement of air quality in CPUA. The data include the hourly monitoring values of $PM_{2.5}$ from the 29 aforementioned cities. Due to the absence of the national ambient monitoring station in JYU, the $PM_{2.5}$ concentrations in JYU were represented by the average $PM_{2.5}$ concentrations from its surrounding cities (JCH, JZU, LYA, SMX, and YCH). All the data were collected from the Data Centre of the PRC Ministry of Ecology and Environment (http://datacenter.mep.gov.cn) and the National Urban Air Quality Real-Time Publishing Platform, China Environmental Monitoring Station (http://106.37.208.233:20035/). At national ambient monitoring stations, the mass concentration of $PM_{2.5}$ is measured by using the beta absorption method and micro oscillating balance method. Daily, monthly, seasonal (spring: March to May, summer: June to August, autumn: September to November, winter: January, February, and December), and annual mean $PM_{2.5}$ concentrations for the cities and urban agglomerations were obtained according to the arithmetic mean method.

Spatiotemporal variation analysis methods

Empirical orthogonal function analysis

The empirical orthogonal function (EOF), which is a form of principal component analysis, can be used to decompose space–time data into a set of orthogonal standing signals (Xu et al. 2019). EOF detects both the spatial and temporal patterns of variability and measures the contribution of each pattern. A matrix X_{mn} (m represents the number of sites, n represents sampling time) can be decomposed into the sum of the product of the orthogonal space matrix V and the orthogonal time matrix T by EOF:

$$X_{mn} = VT = \begin{pmatrix} v_{11} & \cdots & v_{1n} \\ \vdots & \ddots & \vdots \\ v_{m1} & \cdots & v_{mn} \end{pmatrix} \begin{pmatrix} t_{11} & \cdots & t_{1n} \\ \vdots & \ddots & \vdots \\ t_{m1} & \cdots & t_{mn} \end{pmatrix} \quad (1)$$

$$XX^T = VTT^TV^T = V\Lambda V^T \quad (2)$$

where the superscript T represents the transpose of the matrix, Λ is a diagonal matrix composed of the eigenvalues of the matrix, and V is a matrix composed of the matrix eigenvectors.

Thus, the time coefficient can be defined as:

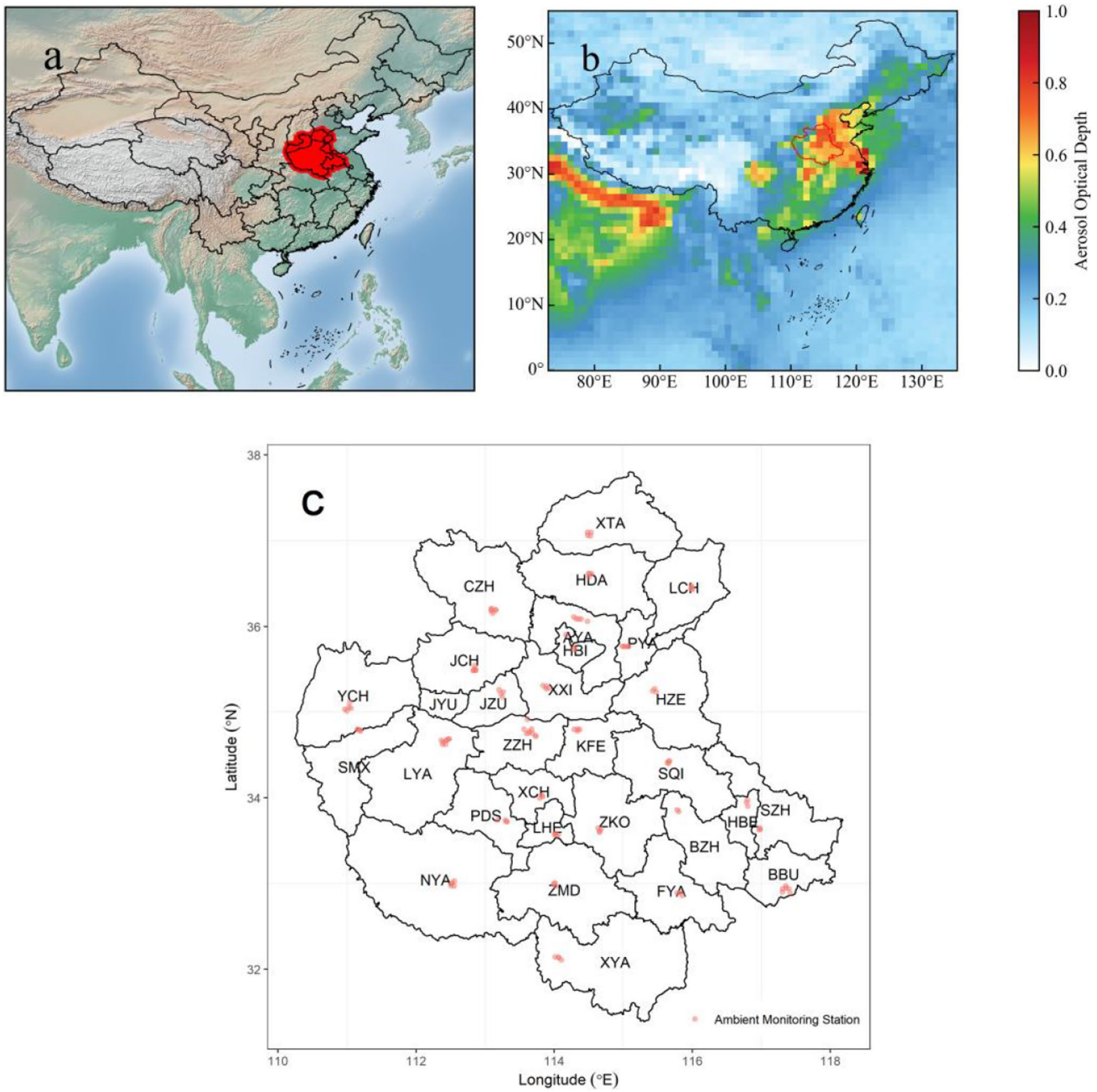

Fig. 1 **a** Location of the Central Plains Urban Agglomeration (CPUA) in China, **b** The mean aerosol optical depth (AOD) in China during 2017. The AOD values were retrieved from the MYD04_L2_C6 product. **c** Cities of CPUA (AYA: Anyang, BBU: Bengbu, BZH: Bozhou, CZH: Changzhi, FYA: Fuyang, HBE: Huaibei, HBI: Hebi, HDA: Handan, HZE: Heze, JCH: Jincheng, JYU: Jiyuan, JZU: Jiaozuo, KFE: Kaifeng, LCH: Liaocheng, LHE: Luohe, LYA: Luoyang, NYA: Nanyang, PDS: Pingdingshan, PYA: Puyang, SMX: Sanmenxia, SQI: Shangqiu, SZH: Suzhou, XCH: Xuchang, XTA: Xingtai, XXI: Xinxiang, XYA: Xinyang, YCH: Yuncheng, ZKO: Zhoukou, ZMD: Zhumadian, ZZH: Zhengzhou)

$$T = V^T X \tag{3}$$

In this research, we use the EOF analysis method to decompose the monthly $PM_{2.5}$ concentrations of the CPUA.

Calculation of centroid migration

The centroid migration of $PM_{2.5}$ concentration in a region, namely the arithmetic mean position of all the points, can reflect the development characteristics on a spatiotemporal

scale, which can help policy-makers better understand highly polluted areas (Jiang et al. 2020; Su et al. 2020). The $PM_{2.5}$ pollution centroid of the CPUA is expressed as follows:

$$X = \frac{\sum_{i=1}^{n} X_i P_i}{\sum_{i=1}^{n} P_i} Y = \frac{\sum_{i=1}^{n} Y_i P_i}{\sum_{i=1}^{n} P_i} \tag{4}$$

where X and Y denote the longitude and latitude coordinates of the centroid for the observed $PM_{2.5}$, respectively. X_i and Y_i are the longitude and latitude of the centroid of city i, respectively. P_i represents the mass concentration of $PM_{2.5}$ in city i, and n is the city number of the CPUA, i.e. 30.

Global and local spatial autocorrelation analysis

The spatial distribution of $PM_{2.5}$ involves complex spatiotemporal and geospatial processes. Previous studies indicated that $PM_{2.5}$ pollution displays some spatial autocorrelation in geographical space (Cheng et al. 2017; Shen et al. 2019; Liu et al. 2017; Ye et al. 2018). In this study, the global Moran's I was employed to discuss the degree of global autocorrelation of $PM_{2.5}$ in the CPUA, and the local Moran's I was used to determine the local spatial autocorrelation and agglomeration patterns. The global Moran's I is expressed as:

$$I_{\text{Global}} = \frac{\sum_{i=1}^{n} \sum_{j \neq i}^{n} W_{ij} \left(x_i - \bar{x}\right) \left(x_j - \bar{x}\right)}{S^2 \sum_{i=1}^{n} \sum_{j \neq i}^{n} W_{ij}} \tag{5}$$

where n represents the number of cities; x_i, x_j is the observed $PM_{2.5}$ of spatial location i, j; $\bar{x} = \frac{1}{n} \sum_{i=1}^{n} x_i$; *and* S denotes the standard deviation of the samples. In the calculation, the Rook contiguity matrix was used to determine the spatial weight between cities W_{ij}.

The Z value was used to test the significance of spatial autocorrelation and is calculated as follows:

$$Z = \frac{I - E(I)}{\sqrt{VAR(I)}} \tag{6}$$

where $E(I)$ and $VAR(I)$ are the expected value and variance of Moran's I, respectively.

The scope of I_{Global} is [-1, 1], and the higher the absolute value is, the stronger the spatial agglomeration. A positive (negative) value of I_{Global} suggests a positive (negative) correlation, while an I_{Global} of 0 indicates no spatial autocorrelation.

The local Moran's I can reveal the features of an urban spatial agglomeration within a region and is calculated as:

$$I_{\text{Local}} = \frac{x_i - \bar{x}}{S^2} \sum_{j=1, j \neq i}^{n} W_{ij} \left(x_j - \bar{x}\right) \tag{7}$$

where x_i, x_j, S^2, $\bar{x}$, W_{ij} are the same as above. Based on the calculated I_{Local}, the spatial association modes can be classified into four types (Su et al. 2020): high-high clustering type (hereinafter HH), low-low clustering type (LL), low–high clustering type (LH), and high-low clustering type (HL). In this study, the HH (LL) type suggests that cities with high (low) $PM_{2.5}$ concentrations are surrounded by others with high (low) $PM_{2.5}$ concentrations. The LH (HL) type suggests that cities with low (high) $PM_{2.5}$ concentrations are surrounded by others with high (low) $PM_{2.5}$ concentrations. I_{Local} that fails the significance test is classified as not significant.

Kernel density estimation

Kernel density estimation was employed to determine the $PM_{2.5}$ density function. Kernel density estimator is defined as:

$$f(x) = \frac{1}{nh} \sum_{i=1}^{n} K\left(\frac{x_i - x}{h}\right) \tag{8}$$

where n denotes the number of samples, h is the bandwidth, and K is the kernel weighting function. As in previous studies (Jiang et al. 2020), the Epanechnikov kernel and Silverman's bandwidth were used in the present study.

Pollution transport analysis

Backward trajectory

Backward trajectory analysis can be used to identify the potential transport pathways of air masses (Liu et al. 2021). Using the Hybrid Single Particle Lagrangian Integrated Trajectory (HYSPLIT) model (Stein et al. 2015), 72-h back trajectories starting at an arrival level of 100 m from the different cities were calculated in autumn and winter of 2017 ~ 2020. The backward trajectory model was run every hour of the day. About 17,000 trajectories were obtained. FNL global analysis data were obtained from the National Centre for Environmental Prediction's Global Data Assimilation System (GDAS) wind field reanalysis (http://www.arl.noaa.gov/) to drive the HYSPLIT model. Then, the backward trajectories having similar geographic origins and histories were classified by k-means clustering (Stunder, 1996).

Potential sources analysis

The potential source contribution function (PSCF) is a conditional probability describing trajectories with pollutant concentrations larger than a given threshold passing through the receptor site (Liu et al. 2019). PSCF is defined as:

$$PSCF_{ij} = \frac{m_{ij}}{n_{ij}} \tag{9}$$

where n_{ij} denotes the total number of trajectory endpoints falling in the ijth cell, and m_{ij} is the number of trajector endpoints with pollutant concentrations higher than the threshold criterion in the same cell. The uncertainty of PSCF increases when n_{ij} is too small. Therefore, a weighting function W_{ij} is multiplied into the PSCF value to reduce the uncertainty (Zhang et al. 2017; Liu et al. 2019). W_{ij} is described as follows:

$$W_{ij} = \begin{cases} 1.00, 3n_{ave} < n_{ij} \\ 0.70, 1.5n_{ave} < n_{ij} \le 3n_{ave} \\ 0.40, n_{ave} < n_{ij} \le 1.5n_{ave} \\ 0.17, n_{ij} \le n_{ave} \end{cases} \quad (10)$$

where n_{ave} denotes the average number of endpoints in each grid cell. In this study, the trajectories associated with hourly $PM_{2.5}$ concentrations were used for PSCF analysis, with the threshold criterion being set at 75 μg/m^3.

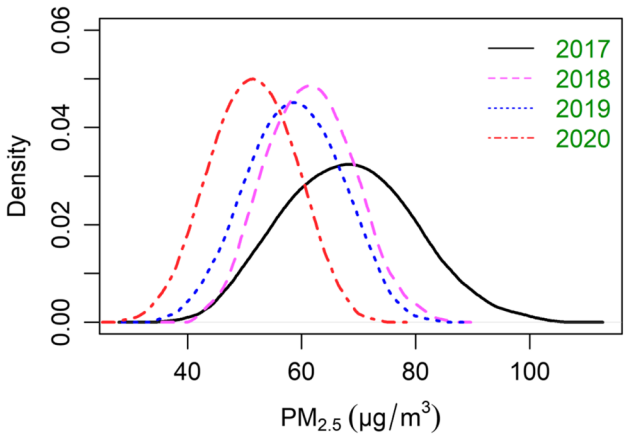

Fig. 2 Kernel density estimates of annual mean $PM_{2.5}$ concentrations from 2017 to 2020

Spatiotemporal variations of $PM_{2.5}$ pollution

Temporal variations of $PM_{2.5}$ pollution

Annual variation

Overall, the $PM_{2.5}$ concentrations of CPUA decreased gradually. From 2017 to 2020, the yearly mean concentrations of $PM_{2.5}$ were 68.3, 61.5, 58.7, and 51.5 μg/m^3. The annual $PM_{2.5}$ concentration was reduced by 24.7% in the 4 years. This suggests that drastic measures aimed at improving air quality in CPUA, e.g. pollution emissions reduction, coal combustion control, and clean energy use, worked well. Notably, the reductions in anthropogenic emissions due to stringent quarantine and lockdown measures during the COVID-19 pandemic in 2020 could dramatically improve the air quality in CPUA. Du et al. (2021) revealed that $PM_{2.5}$ in Zhengzhou decreased by 19% in response to the COVID-19

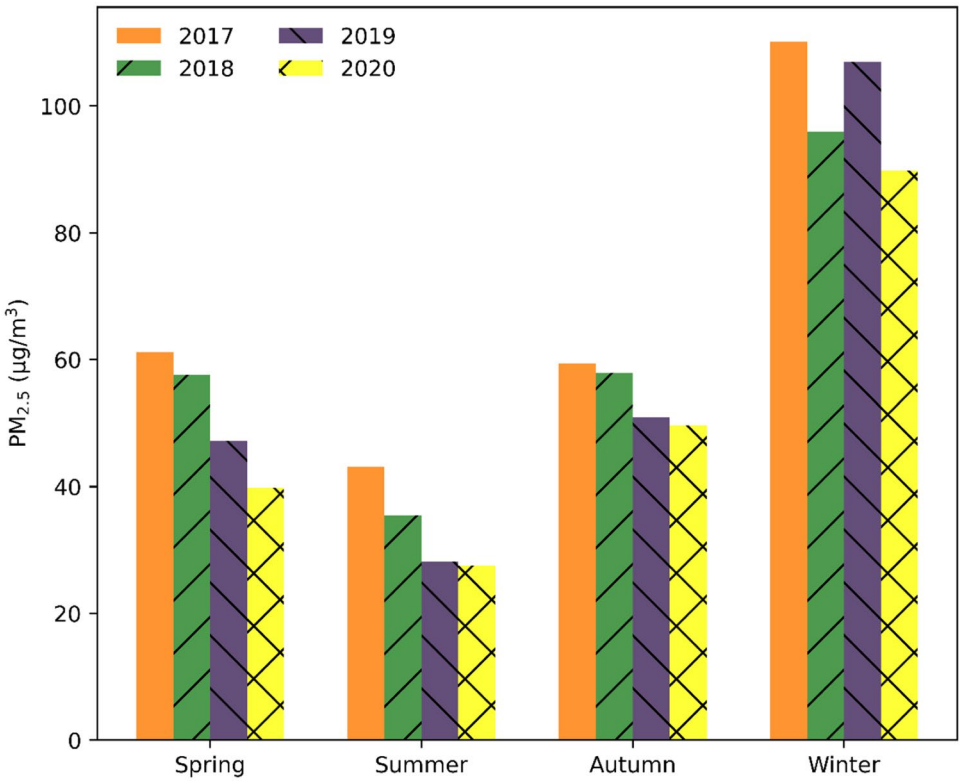

Fig. 3 Seasonal average values of $PM_{2.5}$ concentrations from 2017 to 2020

lockdown. However, it still significantly exceeds the China National Ambient Air Quality Standards II (CAAQS grade I; 35 μg/m^3). The estimated kernel density of annual mean $PM_{2.5}$ concentrations is displayed in Fig. 2. From 2017 to 2020, the peak kernel density curves steepened and gradually moved to the left, demonstrating that concentrations of $PM_{2.5}$ decreased in most cities of the CPUA. Obviously, the area covered by density curves decreased with time at $PM_{2.5}$ concentrations ranging from 60 to 80 μg/m^3, which indicated that city reduction with high $PM_{2.5}$ concentrations benefitted $PM_{2.5}$ pollution alleviation in CPUA.

Seasonal variation

The seasonal means of $PM_{2.5}$ concentrations from 2017 to 2020 are shown in Fig. 3. $PM_{2.5}$ mass concentrations exhibited seasonal variation, with the highest concentration in winter (100.8 μg/m^3, 4-year average), followed by autumn (54.4 μg/m^3) and spring (51.4 μg/m^3), and the lowest in summer (33.5 μg/m^3). This variation is similar to other cities in North China (Shen et al. 2020). In winter, less precipitation leads to weakened wet scavenging. Meanwhile, weak winds and shallow planetary boundary layer heights cause a stable atmospheric structure, which is adverse to the dilution and diffusion of pollution (Wang et al. 2019; Fan et al. 2021). In addition, most of the cities in the CPUA need coal burning for heating in winter, emitting massive air anthropogenic pollutants (Wang et al. 2007). Under the coupling effect of the factors mentioned above, the CPUA suffers from serious $PM_{2.5}$ pollution in winter. The highest decrements in $PM_{2.5}$ concentration appeared in summer, with a reduction of 36%, from 43.1 μg/m^3 in 2017 to 27.5 μg/m^3 in 2020. In contrast, the $PM_{2.5}$ concentration decreased by 18.4%, from 110.1 μg/m^3 in 2017 to 89.8 μg/m^3 in 2020 in winter. In the winter of 2019, the $PM_{2.5}$ concentration even increased. This indicates that $PM_{2.5}$ reduction measures taken in winter need to be more intensive than those in other seasons.

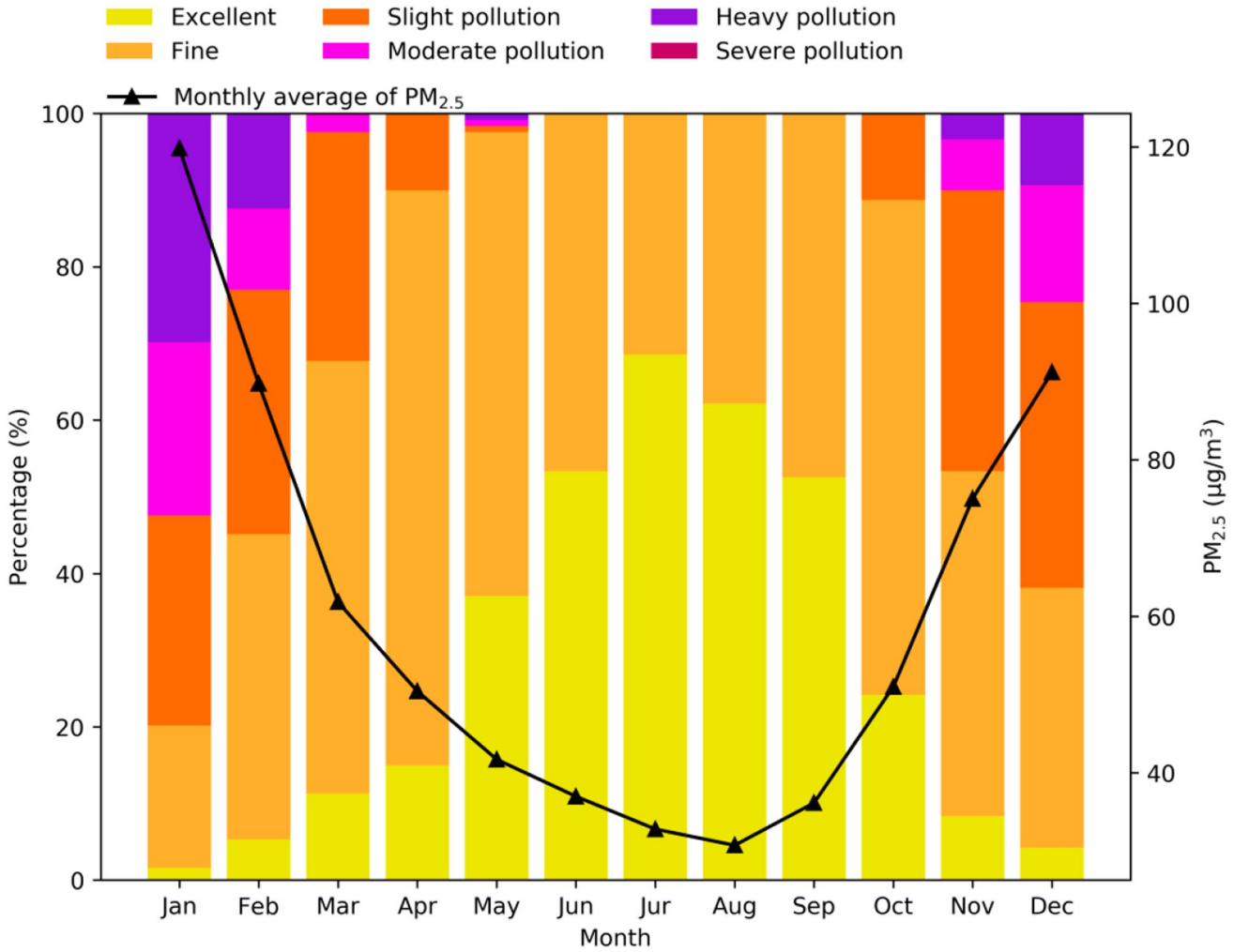

Fig. 4 Monthly average values of $PM_{2.5}$ concentrations from 2017 to 2020

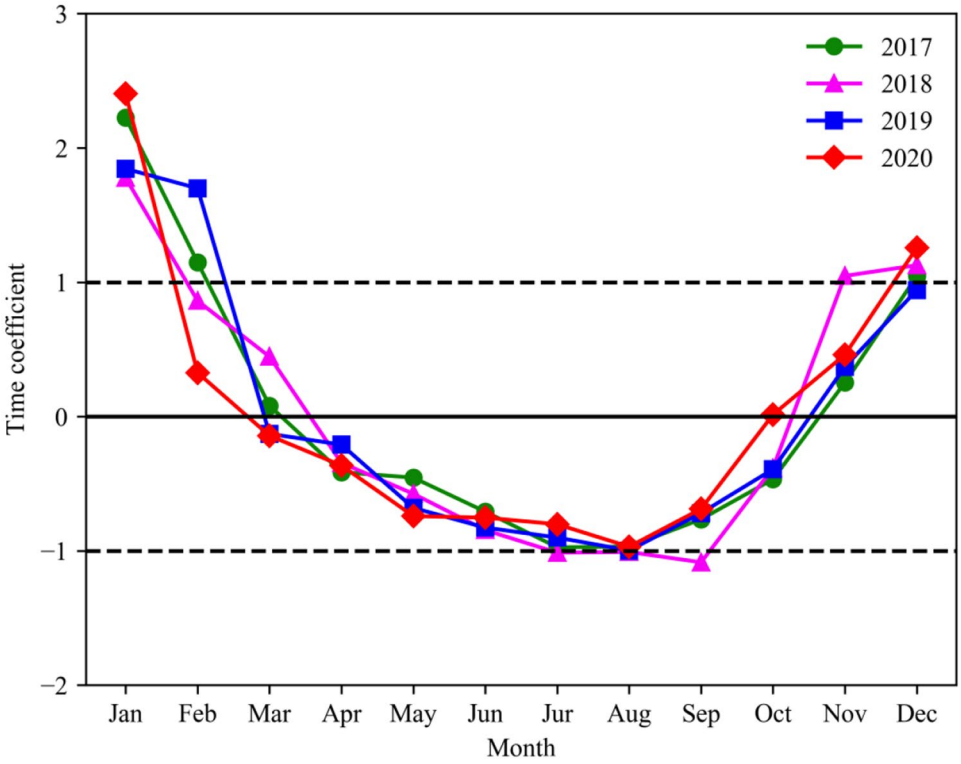

Fig. 5 Time coefficients of the monthly average $PM_{2.5}$ concentrations from 2017 to 2020

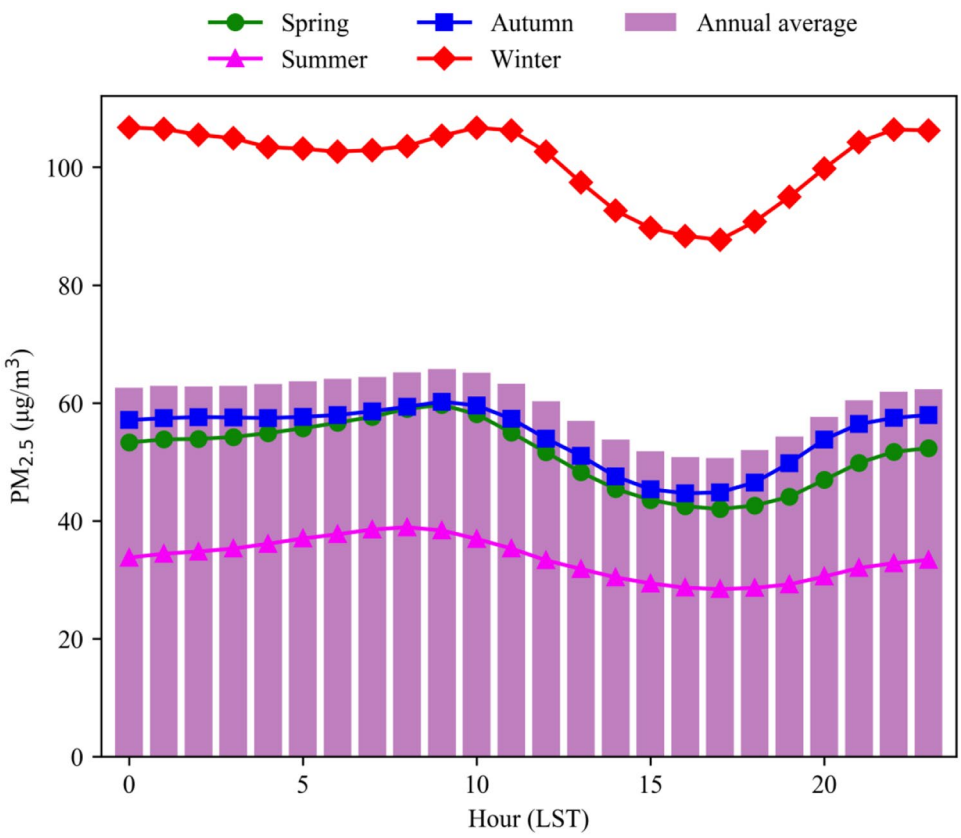

Fig. 6 Diurnal average values of $PM_{2.5}$ concentrations from 2017 to 2020

Monthly variation

The monthly variations in $PM_{2.5}$ concentrations in the CPUA from 2017 to 2020 are illustrated in Fig. 4. According to the daily $PM_{2.5}$ concentrations, the classification categories were designated as follows: excellent ($PM_{2.5} \leq 35$ μg/m^3), fine ($35 < PM_{2.5} \leq 75$ μg/m^3), slight pollution ($75 < PM_{2.5} \leq 115$ μg/m^3), moderate pollution ($115 < PM_{2.5} \leq 150$ μg/m^3), heavy pollution ($150 < PM_{2.5} \leq 250$ μg/m^3), and severe pollution ($PM_{2.5} > 250$ μg/m^3). The monthly average $PM_{2.5}$ concentrations exhibited a U-shaped trend, with the highest value in January (119.8 μg/m^3) and the lowest value in August (30.7 μg/m^3). In June, July, August, and September, the daily $PM_{2.5}$ concentrations were all under 75 μg/m^3. In January, February, November, and December, the frequencies of days with heavy pollution were 29.8%, 12.4%, 3.3%, and 9.3%, respectively.

The EOF method was employed to decompose the monthly mean $PM_{2.5}$ concentrations of the cities in the CPUA. The first EOF model accounted for 92.1% of the total variance, which suggested that the decomposition of

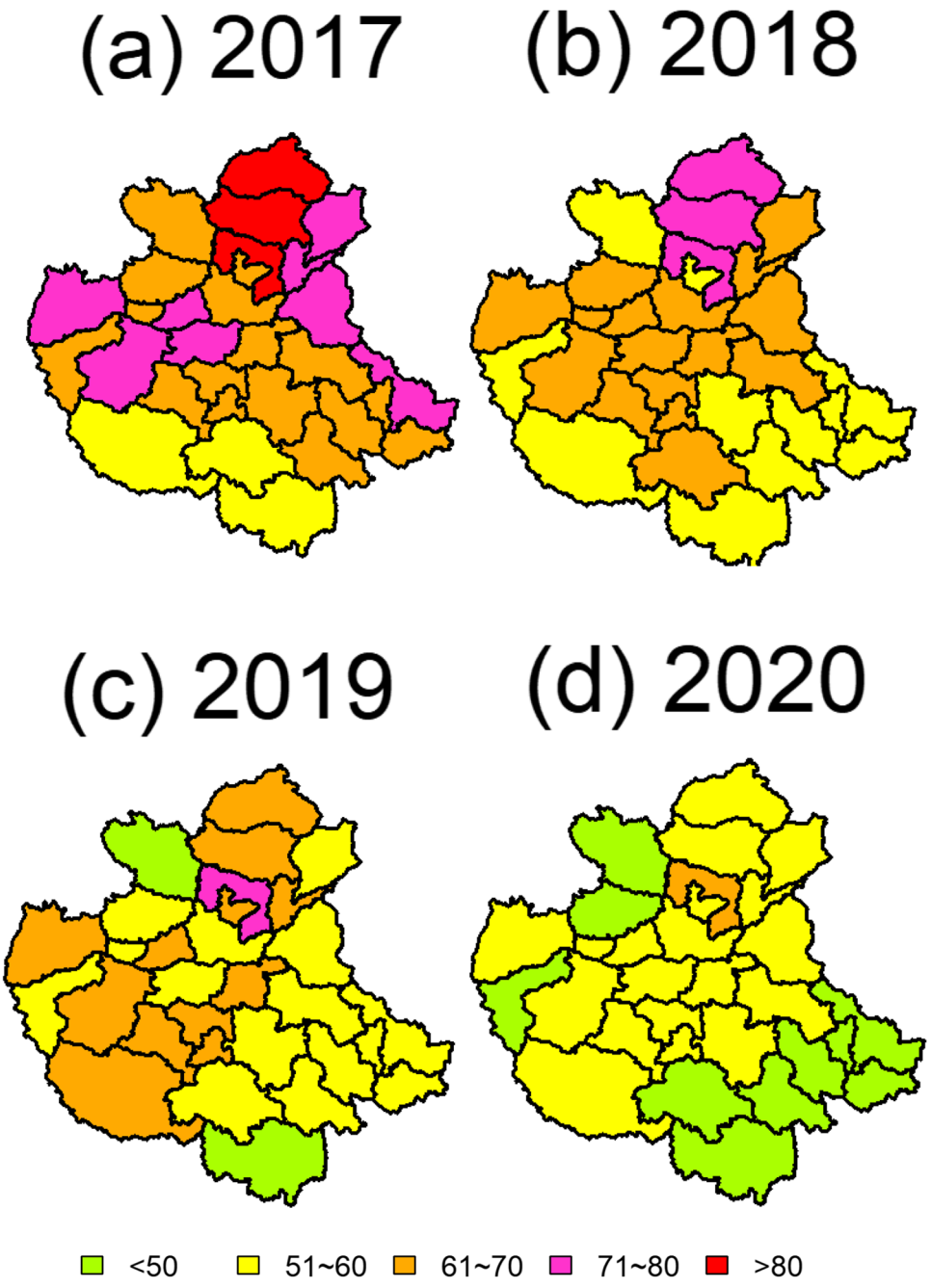

Fig. 7 Spatial distributions of yearly average values of $PM_{2.5}$ concentrations from 2017 to 2020

$PM_{2.5}$ was successful. In this study, we paid more attention to time coefficients decomposed by EOF, which can reflect the variation trend of monthly $PM_{2.5}$ concentrations in CPUA. The decomposed time coefficients were standardized to have zero mean and unit variance (Jiang et al. 2020). As shown in Fig. 5, the time coefficients in the 4 years all displayed a U-shaped curve, which is similar to the variation trend of $PM_{2.5}$ mass concentrations. In winter, most of the time coefficients are out of the scope of [-1, 1], indicating extreme events, namely high $PM_{2.5}$ pollution. In February, there were obviously fewer extreme events in 2020 than in other years, which could be due to the lockdown for dealing with the outbreak of coronavirus disease 2019 (COVID-19) (Silver et al. 2020; Kwak et al. 2021).

Diurnal variation

As displayed in Fig. 6, the diurnal variations in $PM_{2.5}$ in the four seasons had low concentrations during the daytime and high concentrations during the nighttime, which was related to the diurnal changes in the boundary layer (Liu et al. 2021). The $PM_{2.5}$ concentration had a peak at 9:00 in spring, 8:00 in summer, 10:00 in autumn, and 11:00 in winter, corresponding to anthropogenic emissions in rush hours (Wang et al. 2016). From 00:00 to 6:00, the $PM_{2.5}$ concentration decreased slowly in winter but increased in other seasons. $PM_{2.5}$ exhibited the lowest concentrations at 16:00 ~ 17:00, which could be related to the highest planetary boundary layer height (PBLH) occurring at this time.

Spatial distributions of $PM_{2.5}$ pollution

Spatial Variation of $PM_{2.5}$

Figure 7 displays the distribution of $PM_{2.5}$ in CPUA. It was clear that the spatial distribution of $PM_{2.5}$ was heterogeneous. In 2017, the annual mean $PM_{2.5}$ concentrations of Handan, Anyang, Xingtai, and Jiaozuo exceeded 75 μg/m^3. These highly polluted cities are all characterized by industry. In addition, Luoyang, Suzhou, Liaocheng, Yuncheng, Zhengzhou, Heze, and Puyang also have higher $PM_{2.5}$ concentrations. $PM_{2.5}$ concentrations presented a gradual decline over time, presenting a convergence trend. From 2017 to 2020, cities with $PM_{2.5}$ concentrations above 60 μg/m^3 accounted for 89.7%, 62.1%, 44.8%, and 34.5% of all cities in the CPUA, respectively. The three cities with the highest reduction in $PM_{2.5}$ concentration were Suzhou (37.2%), Xingtai (34.2%), and Handan (33.6%) from 2017 to 2020. In 2020, cities in the southeastern CPUA, e.g. Xinyang, had low $PM_{2.5}$ concentration levels.

Centroid migration route

The centroids of the annual mean $PM_{2.5}$ concentration from 2017 to 2020 were located at the borders between

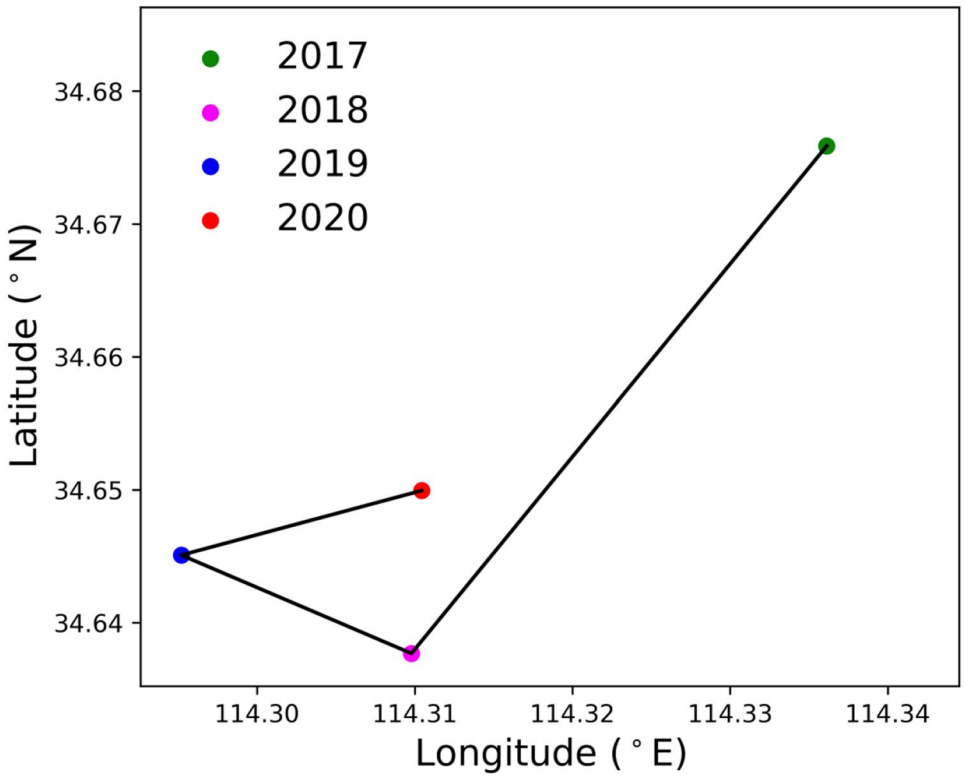

Fig. 8 Centroid migration route of PM2.5 from 2017 to 2020

western Kaifeng and eastern Zhengzhou (Fig. S1). The $PM_{2.5}$ pollution centroids were also located in the southeastern CPUA geographical centroid, with a distance of approximately 10 km. The centroid of $PM_{2.5}$ concentration exhibited a trend of moving towards the west from 2017 to 2019 (Fig. 8), which indicates that the west CPUA had more serious $PM_{2.5}$ pollution. The $PM_{2.5}$ pollution centroids in 2018 ~ 2020 were all in southern 2017, which may be related to the sharp reduction in $PM_{2.5}$ in Xingtai and Handan.

Spatial autocorrelation of $PM_{2.5}$ concentrations

To further discuss the spatial characteristics of $PM_{2.5}$ spatial correlation, the global Moran's I was calculated. Moran's I statistics from 2017 to 2020 are 0.34, 0.20, 0.28, and 0.26, respectively, passing the significance test, which indicates that $PM_{2.5}$ concentrations have a positive spatial autocorrelation in CPUA. This suggests that $PM_{2.5}$ in a city can be affected by its neighbouring cities. Previous studies also indicate that regional transport of $PM_{2.5}$ plays an important role in regional haze episodes (Hu et al. 2021; Wang et al. 2014). Hence, regional joint cooperation

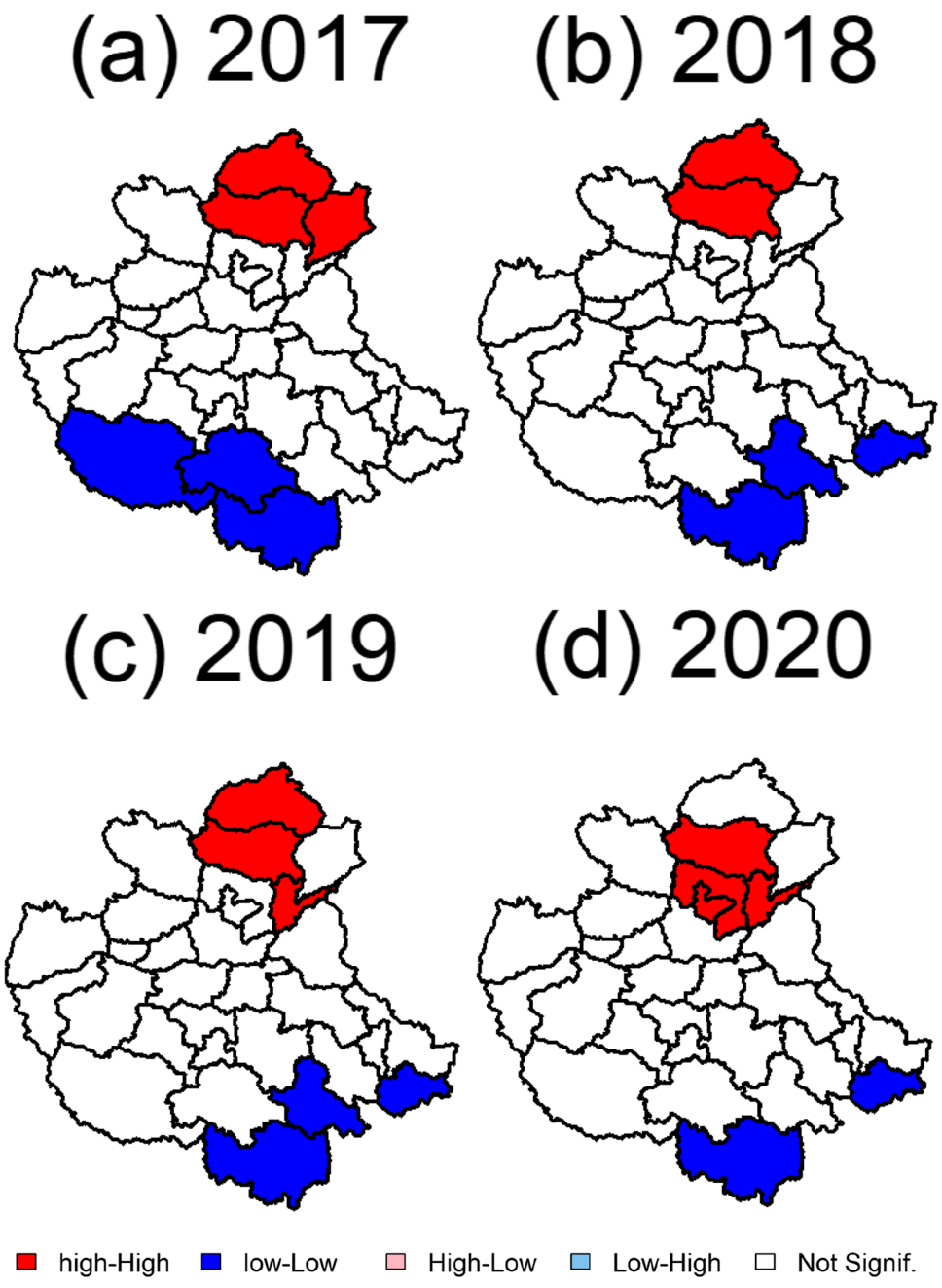

Fig. 9 Spatial agglomeration of $PM_{2.5}$ concentrations in the Central Plains Urban Agglomeration from 2017 to 2020

across cities is necessary to improve air quality. In general, the global Moran's I decreased over time, which indicated the weakening spatial autocorrelation of $PM_{2.5}$. In summer, the global Moran's I of $PM_{2.5}$ concentrations was higher than that in other seasons (Fig. S2). We deduced that in summer, intensive atmospheric activity is conducive to the diffusion and mixing of anthropogenic pollutants, which leads to a relatively homogeneous distribution of $PM_{2.5}$ concentrations. In winter, the lowest global Moran's I suggested that $PM_{2.5}$ heterogeneity increased, which was related to the stable atmosphere and local emission sources. As shown in Fig. S3, the global Moran's I increased gradually during 02:00 ~ 9:00 and increased sharply during 9:00 ~ 13:00 due to the enhanced solar radiation. Then, the global Moran's I decreased continuously, implying that the interplay of $PM_{2.5}$ pollution between cities in the CPUA decreased.

Local spatial autocorrelation analysis was employed to identify the distribution and agglomeration patterns of $PM_{2.5}$ pollution in each city of the CPUA. As displayed in Fig. 9, the agglomeration patterns displayed varying but similar spatial distributions over time. Overall, the most polluted cities were distributed in northern CPUA, which are all industrial cities with intensive anthropogenic emissions, forming $PM_{2.5}$ pollution clusters. Cities with good air quality were located in the southern CPUA, which has abundant precipitation and small anthropogenic emissions, forming a low-low (LL) agglomeration type of $PM_{2.5}$ concentration. The area with high-high (HH) agglomeration of $PM_{2.5}$ pollution tended to migrate southward. In 4 years, Handan and Xinyang were the high-high (HH) and low-low (LL) $PM_{2.5}$ concentration centres, respectively. In summer, the proportion of LL and HH clusters among CPUA was the largest in the four seasons (Fig. S4). In winter, this proportion was the smallest, which indicated a decreasing spatial autocorrelation among CPUA.

Regional transportation of $PM_{2.5}$

Backward trajectory analysis

To investigate the $PM_{2.5}$ transportation of CPUA, three typical cities, namely Xingtai (the most $PM_{2.5}$ polluted city), Zhengzhou (the capital of Henan province and the largest city in CPUA), and Xinyang (the lowest $PM_{2.5}$ polluted city), were selected to calculate the backward trajectories in autumn and winter for each year. As displayed in Fig. 10a, all trajectories of Xingtai were classified into four categories, C1 (28.3%), C2 (30.3%), C3 (24.4%), and C4 (17.1%), corresponding to $PM_{2.5}$ concentrations of 110.5, 107.8, 79.7, and 81.6 μg/m^3, respectively. C1 started in Inner Mongolia and passed through northern Shanxi Province. C2, a short-distance transport, crossed northwestern Shandong Province and southern Hebei Province. This suggested that the northern CPUA could be influenced by $PM_{2.5}$ transmission from northwestern Shandong, southern Hebei, and northern Shanxi provinces. The trajectories of Zhengzhou were also

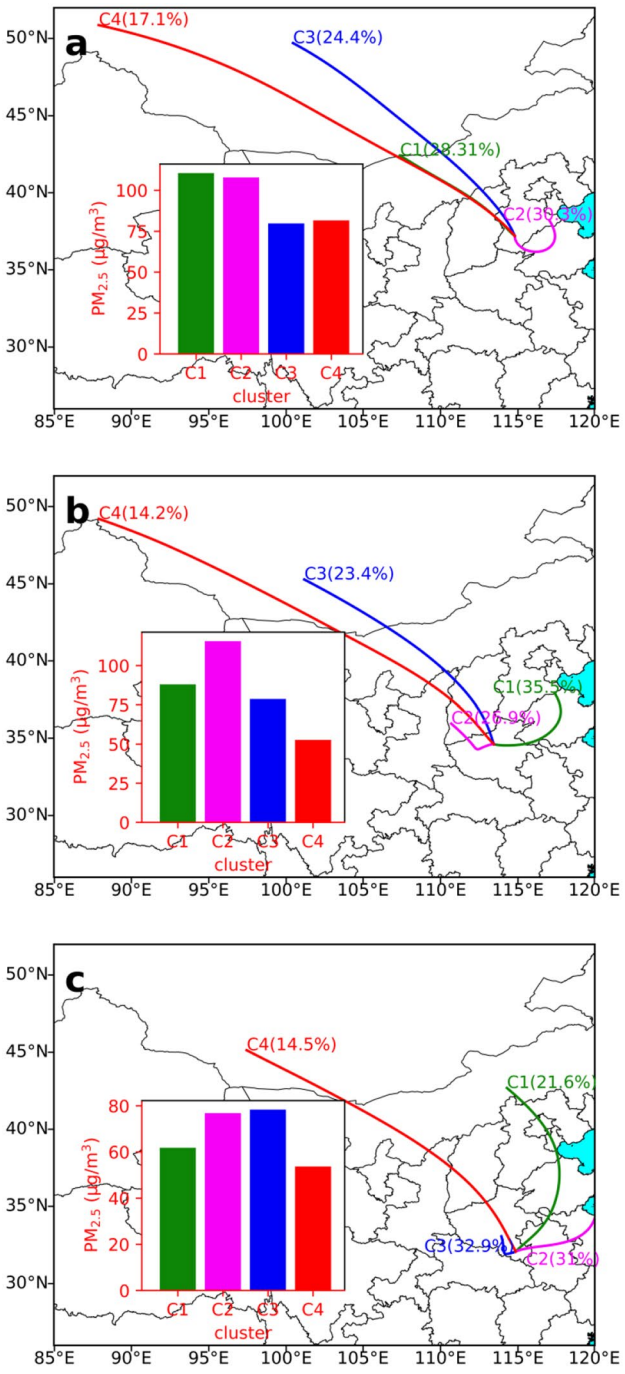

Fig. 10 Back trajectory clusters and the mean mass concentration of $PM_{2.5}$ under the corresponding cluster in **a** Xingtai, **b** Zhengzhou, and **c** Xinyang

classified into four categories (Fig. 10b), among which C2 (26.9%), C3 (23.4%), and C4 (14.2%) came from northwestern Zhengzhou, and C1 (35.5%) originated from northeastern Zhengzhou. C2, passing through southwestern Shanxi and northwestern Henan provinces, was the most polluted, with a $PM_{2.5}$ concentration of 115.6 μg/m^3. The $PM_{2.5}$ concentrations corresponding to C1, C3, and C4 were 88.0, 78.6, and 52.7 μg/m^3, respectively; the $PM_{2.5}$ concentrations of the four trajectory clusters for Xinyang were lower than those of Xingtai and Zhengzhou (Fig. 10c). C3 (32.9%), the most polluted cluster with a $PM_{2.5}$ concentration of 78.3 μg/m^3, started in southern Henan Province and moved a short distance before arriving at Xinyang. C2 (31.0%) was the second $PM_{2.5}$ pollution (76.8 μg/m^3), crossing northern Anhui Province. This indicated that Xinyang could be influenced by southern Henan and northern Anhui provinces. In three typical cities of the CPUA (Xingtai, Zhengzhou, and Xinyang), all short-distance trajectories correspond to high $PM_{2.5}$ concentrations, which suggested that internal transport played a key role in $PM_{2.5}$ pollution over the CPUA. Meanwhile, the $PM_{2.5}$ transport crossing region was important as well. Air masses starting from the northwest and having long-distance movement all corresponded to low $PM_{2.5}$ concentrations.

Potential sources

The PSCF model was used to identify the potential source areas for $PM_{2.5}$ (> 75 μg/m^3) in Xingtai, Zhengzhou, and Xinyang. The study domain in the three cities was 85 ~ 120° E, 26 ~ 52° N, with a spatial resolution of

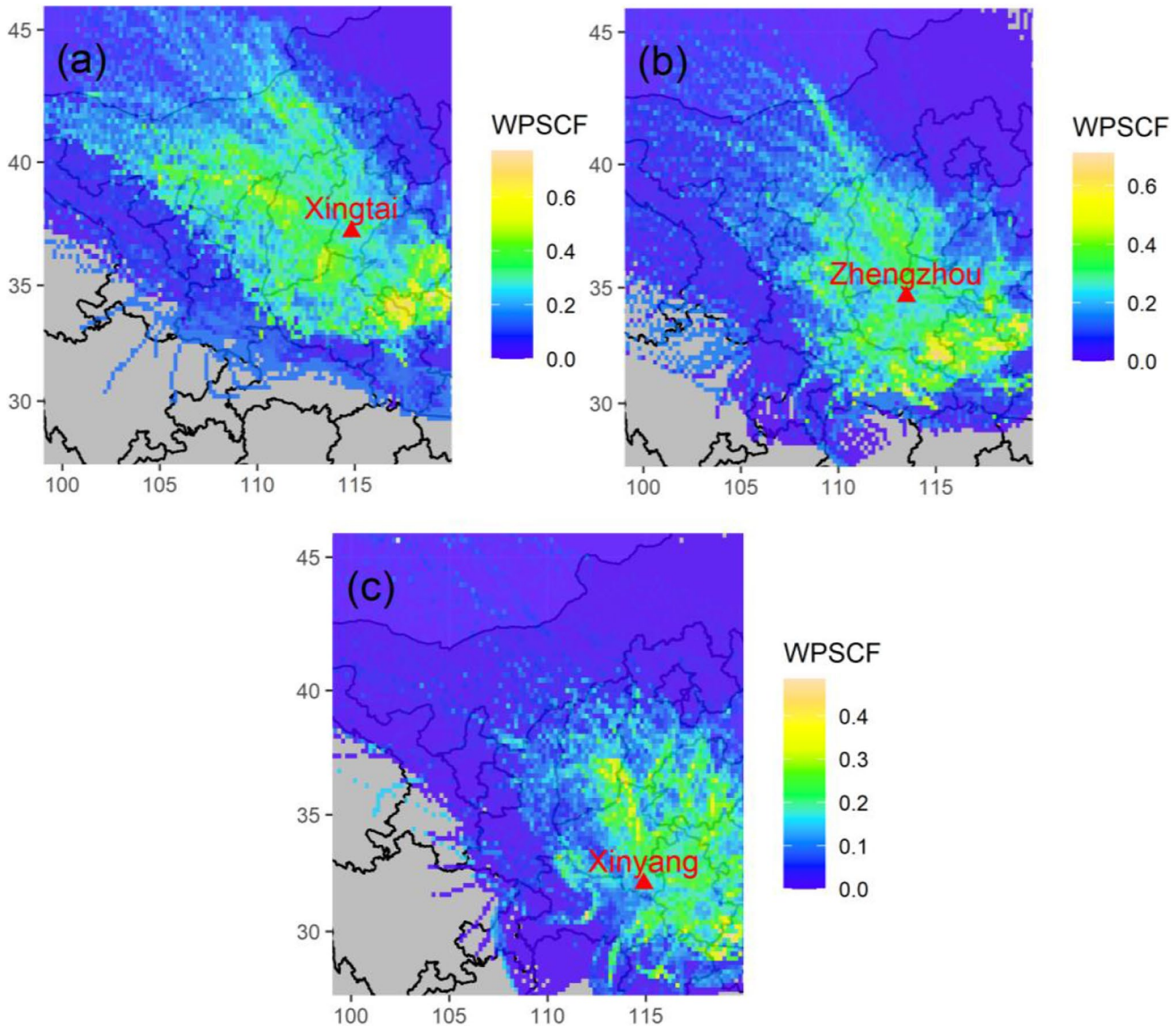

Fig. 11 Results of PSCF analysis for $PM_{2.5}$ concentration above 75 μg/m^3 in **a** Xingtai, **b** Zhengzhou, and **c** Xinyang

0.2° × 0.2°. As shown in Fig. 11a, cells with high WPSCF values were mainly located in Lvliang, Changzhi, southeastern Shandong Province, and northern Anhui Province, which suggested that those regions were strong potential source areas influencing the $PM_{2.5}$ concentration of Xingtai. For Zhengzhou (Fig. 11b), the strong potential source areas mainly included southeastern Henan Province, northern Anhui Province, and northeastern Hubei Province. In Xinyang (Fig. 11c), there were fewer grids with WPSCF values above 0.5 than in the other two cities due to the good air quality in Xinyang. The grids of WPSCF greater than 0.4 were mainly located at Changzhi, Anyang, Xinxiang, and Linyi. In summary, potential source analysis for three cities all indicated that $PM_{2.5}$ transmission in CPUA and cross-boundaries was important, emphasizing the necessity of joint efforts among cities and regions.

Conclusions

In this study, multiple transdisciplinary methods, including geographical analysis, spatial statistics, and potential source analysis, were employed to investigate the spatial and temporal variations and the potential geographical source of $PM_{2.5}$ in the CPUA. During 2017 ~ 2020, the annual mean concentrations of $PM_{2.5}$ were 68.3, 61.5, 58.7, and 51.5 μg/m^3, respectively. The kernel density estimation results suggested that city reduction with high $PM_{2.5}$ concentrations benefitted $PM_{2.5}$ pollution alleviation in the CPUA. $PM_{2.5}$ exhibited the highest concentration in winter (100.8 μg/m^3, 4-year average) and the lowest concentration in summer (33.5 μg/m^3). From 2017 to 2020, the $PM_{2.5}$ concentration decreased 36% in summer and 18.4% in winter. $PM_{2.5}$ concentrations showed a U-shaped trend with month, with the highest value appearing in January (119.8 μg/m^3) and the lowest in August (30.7 μg/m^3). The time series of $PM_{2.5}$ concentrations were decomposed by EOF, and the results indicated that high $PM_{2.5}$ pollution mainly occurred in winter. Small different diurnal variations in $PM_{2.5}$ were observed over the season due to anthropogenic emissions and PBLH variation. The spatial distribution of $PM_{2.5}$ in CPUA was heterogeneous. The centroid of $PM_{2.5}$ concentration was located in western Kaifeng and moved towards the west over time. The spatial autocorrelation analysis revealed that $PM_{2.5}$ concentrations exhibited a positive spatial autocorrelation in CPUA. The spatial autocorrelation was the strongest in summer and the lowest in winter. In the diurnal variation, the global Moran's I increased during 02:00 ~ 13:00 and then increased. The most polluted cities were distributed in the northern CPUA, forming a high-high agglomeration, and the cities located in the southern CPUA formed a low-low agglomeration. Handan and Xinyang were the centres of high-high and low-low agglomeration, respectively. The HYSPLIT model and PCSF were used to discuss the regional transportation of $PM_{2.5}$ in the CPUA. The results suggested that internal transport played a key role in $PM_{2.5}$ pollution over the CPUA and that the $PM_{2.5}$ cross-boundary of the CPUA was also important. Our findings suggest that drastic measures, including pollution emissions reduction, coal combustion control, and vehicle restriction, are necessarily taken in winter. Joint efforts across cities and regions are needed to further improve the air quality of CPUA.

Supplementary Information The online version contains supplementary material available at https://doi.org/10.1007/s11869-022-01178-z.

Acknowledgements This work was supported by Program for Innovative Research Team (in Science and Technology) in University of Henan Province (Grant No. 22IRTSTHN010) and the Key Science and Technology Research Project of Henan Province of China (Grant No. 18A170013). The authors would like to acknowledge Nanhu Scholars Program for Young Scholars of XYNU.

Funding This work was supported by Program for Innovative Research Team (in Science and Technology) in University of Henan Province (Grant No. 22IRTSTHN010), the Key Science and Technology Research Project of Henan Province of China (Grant No. 18A170013), and the Nanhu Scholars Program for Young Scholars of XYNU.

Data availability The datasets generated during and/or analysed during the current study are available from the corresponding author on reasonable request.

We declare that we have no financial and personal relationships with other people or organizations that can inappropriately influence our work, there is no professional or other personal interest of any nature or kind in any product, service and/or company that could be construed as influencing the position presented in, or the review of, the manuscript entitled "Spatiotemporal variations and sources of $PM_{2.5}$ in the Central Plains Urban Agglomeration, China".

References

Cao JJ, Cui L (2021) Current status, characteristics and causes of particulate air pollution in the Fenwei Plain, China: a review. J Geophys Res Atmos 126, e2020JD034472

Chen ZY, Chen DL, Wen W, Zhuang Y, Kwan MP, Chen B, Zhao B, Yang L, Gao BB, Li RY, Xu B (2019) Evaluating the "2+26" regional strategy for air quality improvement during two air pollution alerts in Beijing: variations in $PM_{2.5}$ concentrations, source apportionment, and the relative contribution of local emission and regional transport. Atmos Chem Phys 19:6879–6891

Cheng ZH, Li LS, Liu J (2017) Identifying the spatial effects and driving factors of urban $PM_{2.5}$ pollution in China. Ecol Indic 82:61–75

Cohen AJ, Brauer M, Burnett R, Anderson HR, Frostad J, Estep K, Balakrishnan K, Brunekreef B, Dandona L, Dandona R, Feigin V, Freedman G, Hubbell B, Jobling A, Kan H, Knibbs L, Liu Y, Martin R, Morawska L, Pope CA, Shin H, Straif K, Shaddick G, Thomas M, van Dingenen R, van Donkelaar A, Vos T, Murray CJL, Forouzanfar MH (2017) Estimates and 25-year trends of the global burden of disease attributable to ambient air pollution: an analysis of data from the global burden of diseases study 2015. Lancet 389:1907–1918

Ding YT, Zhang M, Chen S, Wang WW, Nie R (2019) The environmental Kuznets curve for $PM_{2.5}$ pollution in Beijing-Tianjin-Hebei region of China: a spatial panel data approach. J Clean Prod 220:984–994

Du H, Li J, Wang Z, Yang W, Chen X, Wei Y (2021) Sources of $PM_{2.5}$ and its responses to emission reduction strategies in the Central Plains Economic Region in China: implications for the impacts of COVID-19. Environ Pollut 288: 117783

Fan S, Gao CY, Wang L, Yang Y, Liu Z, Hu B, Wang Y, Wang J, Gao Z (2021) Elucidating roles of near-surface vertical layer structure in different stages of $PM_{2.5}$ pollution episodes over urban Beijing during 2004–2016 Atmos Environ 246

Feng JL, Yu H, Mi K, Su XF, Li Y, Li QL, Sun JH (2018) One year study of $PM_{2.5}$ in Xinxiang City, North China: seasonal characteristics, climate impact and source. Ecotox Environ Safe 154:75–83

Fu XS, Li L, Lei YL, Wu SM, Yan D, Luo XM, Luo H (2020) The economic loss of health effect damages from $PM_{2.5}$ pollution in the Central Plains Urban Agglomeration. Environ Sci Pollut Res 27:25434–25449

Gao JJ, Wang K, Wang Y, Liu SH, Zhu CY, Hao JM, Liu HJ, Hua SB, Tian HZ (2018) Temporal-spatial characteristics and source apportionment of $PM_{2.5}$ as well as its associated chemical species in the Beijing-Tianjin-Hebei Region of China. Environ Pollut 233:714–724

Hu WY, Zhao TL, Bai YQ, Kong SF, Xiong J, Sun XY, Yang QJ, Gu Y, Lu HC (2021) Importance of regional $PM_{2.5}$ transport and precipitation washout in heavy air pollution in the Twain-Hu basin over Central China: observational analysis and WRF-Chem simulation. Sci Total Environ 758:8

Huang RJ, Zhang YL, Bozzetti C, Ho KF, Cao JJ, Han YM, Daellenbach KR, Slowik JG, Platt SM, Canonaco F, Zotter P, Wolf R, Pieber SM, Bruns EA, Crippa M, Ciarelli G, Piazzalunga A, Schwikowski M, Abbaszade G, Schnelle-Kreis J, Zimmermann R, An ZS, Szidat S, Baltensperger U, El Haddad I, Prevot ASH (2014) High secondary aerosol contribution to particulate pollution during haze events in China. Nature 514:218–222

Jiang N, Yin SS, Guo Y, Li JY, Kang PR, Zhang RQ, Tang XY (2018) Characteristics of mass concentration, chemical composition, source apportionment of $PM_{2.5}$ and PM_{10} and health risk assessment in the emerging megacity in China. Atmos Pollut Res 9:309–321

Jiang L, He SX, Zhou HF (2020) Spatio-temporal characteristics and convergence trends of $PM_{2.5}$ pollution: a case study of cities of air pollution transmission channel in Beijing-Tianjin-Hebei Region, China J Clean Prod 256:13

Kwak KH, Han BS, Park K, Moon S, Jin HG, Park SB, Baik JJ (2021) Inter- and intra-city comparisons of $PM_{2.5}$ concentration changes under COVID-19 social distancing in seven major cities of South Korea. Air Qual Atmos Health, pp 1–14

Liang D, Wang YQ, Wang YJ, Ma C (2019) National air pollution distribution in China and related geographic, gaseous pollutant, and socio-economic factors. Environ Pollut 250:998–1009

Liu HM, Fang CL, Zhang XL, Wang ZY, Bao C, Li FZ (2017) The Effect of natural and anthropogenic factors on haze pollution in Chinese cities: a spatial econometrics approach. J Clean Prod 165:323–333

Liu HJ, Tian HZ, Zhang K, Liu SH, Cheng K, Yin SS, Liu YL, Liu XY, Wu YM, Liu W, Bai XX, Wang Y, Shao PY, Luo LN, Lin SM, Chen J, Liu XG (2019) Seasonal variation, formation mechanisms and potential sources of $PM_{2.5}$ in two typical cities in the Central Plains Urban Agglomeration. China Sci Total Environ 657:657–670

Liu XY, Pan XL, Wang ZF, He H, Wang DW, Liu H, Tian Y, Xiang WL, Li J (2020) Chemical characteristics and potential sources of $PM_{2.5}$ in Shahe city during severe haze pollution episodes in the winter. Aerosol Air Qual Res 20:2741–2753

Liu X, Wang M, Pan X, Wang X, Yue X, Zhang D, Ma Z, Tian Y, Liu H, Lei S, Zhang Y, Liao Q, Ge B, Wang D, Li J, Sun Y, Fu P, Wang Z, He H (2021) Chemical formation and source apportionment of $PM_{2.5}$ at an urban site at the southern foot of the Taihang Mountains. J Environ Sci 103:20–32

Ming LL, Jin L, Li J, Fu PQ, Yang WY, Liu D, Zhang G, Wang ZF, Li XD (2017) $PM_{2.5}$ in the Yangtze River Delta, China: chemical compositions, seasonal variations, and regional pollution events. Environ Pollut 223:200–212

Shen Y, Zhang LP, Fang X, Ji HY, Li X, Zhao ZW (2019) Spatiotemporal patterns of recent $PM_{2.5}$ concentrations over typical urban agglomerations in China. Sci Total Environ 655:13–26

Shen FZ, Zhang L, Jiang L, Tang MQ, Gai XY, Chen MD, Ge XL (2020) Temporal variations of six ambient criteria air pollutants from 2015 to 2018, their spatial distributions, health risks and relationships with socioeconomic factors during 2018 in China. Environ Int 137:13

Silver B, He XY, Arnold SR, Spracklen DV (2020) The impact of Covid-19 control measures on air quality in China. Environ Res Lett 15:12

Stein AF, Draxler RR, Rolph GD, Stunder BJB, Cohen MD, Ngan F (2015) Noaa's hysplit atmospheric transport and dispersion modeling system. Bull Amer Meteorol Soc 96:2059–2077

Stunder BJB (1996) An assessment of the quality of forecast trajectories. J Appl Meteorol Climatol 35:1319–1331

Su Y, Lu CY, Lin XQ, Zhong LX, Gao YB, Lei YF (2020) Analysis of spatio-temporal characteristics and driving forces of air quality in the northern coastal comprehensive economic zone. China Sustainability 12:23

Su B, Wu DY, Zhang M, Bilal M, Li YY, Li BL, Atique L, Zhang ZY, Howari FM (2021) Spatio-temporal characteristics of $PM_{2.5}$, PM_{10}, and AOD over the Central Line Project of China's South-North water diversion in Henan Province (China). Atmosphere 12:19

Tian M, Liu Y, Yang FM, Zhang LM, Peng C, Chen Y, Shi GM, Wang HB, Luo B, Jiang CT, Li B, Takeda N, Koizumi K (2019) Increasing importance of nitrate formation for heavy aerosol pollution in two megacities in Sichuan Basin, Southwest China. Environ Pollut 250:898–905

Wang GH, Kawamura K, Zhao X, Li QG, Dai ZX, Niu HY (2007) Identification, abundance and seasonal variation of anthropogenic organic aerosols from a mega-city in China. Atmos Environ 41:407–416

Wang ZF, Li J, Wang Z, Yang WY, Tang X, Ge BZ, Yan PZ, Zhu LL, Chen XS, Chen HS, Wand W, Li JJ, Liu B, Wang XY, Wand W, Zhao YL, Lu N, Su DB (2014) Modeling study of regional severe hazes over Mid-Eastern China in January 2013 and its implications on pollution prevention and control. Sci China-Earth Sci 57:3–13

Wang HL, An JL, Cheng MT, Shen LJ, Zhu B, Li Y, Wang YS, Duan Q, Sullivan A, Xia L (2016) One year online measurements of water-soluble ions at the industrially polluted town of Nanjing, China: Sources, Seasonal and Diurnal Variations. Chemosphere 148:526–536

Wang HF, Li ZQ, Lv Y, Xu H, Li KT, Li DH, Hou WZ, Zheng FX, Wei YY, Ge BY (2019) Observational study of aerosol-induced impact on planetary boundary layer based on lidar and sunphotometer in Beijing. Environ Pollut 252:897–906

Wang S, Wang L, Wang N, Ma S, Su F, Zhang R (2021) Formation of droplet-mode secondary inorganic aerosol dominated the increased $PM_{2.5}$ during both local and transport haze episodes in Zhengzhou, China. Chemosphere 269

Xu H, Xiao ZM, Chen K, Tang M, Zheng NY, Li P, Yang N, Yang W, Deng XW (2019) Spatial and temporal distribution, chemical characteristics, and sources of ambient particulate matter in the Beijing-Tianjin-Hebei region. Sci Total Environ 658:280–293

Xu XH, Zhang TC (2020) Spatial-temporal variability of $PM_{2.5}$ air quality in Beijing, China during 2013–2018. J. Environ. Manage. 262: 10

Yan D, Lei YL, Shi YK, Zhu Q, Li L, Zhang Z (2018) Evolution of the spatiotemporal pattern of $PM_{2.5}$ concentrations in China - a case study from the Beijing-Tianjin-Hebei region. Atmos Environ 183:225–233

Yang S, Ma YL, Duan FK, He KB, Wang LT, Wei Z, Zhu LD, Ma T, Li H, Ye SQ (2018) Characteristics and formation of typical winter haze in handan, one of the most polluted cities in China. Sci Total Environ 613:1367–1375

Ye WF, Ma ZY, Ha XZ (2018) Spatial-temporal patterns of $PM_{2.5}$ concentrations for 338 Chinese cities. Sci Total Environ 631–632:524–533

Zhai SX, Jacob DJ, Wang X, Shen L, Li K, Zhang YZ, Gui K, Zhao TL, Liao H (2019) Fine particulate matter ($PM_{2.5}$) trends in China, 2013–2018: separating contributions from anthropogenic emissions and meteorology. Atmos Chem Phys 19:11031–11041

Zhang YP, Chen J, Yang HN, Li RJ, Yu Q (2017) Seasonal variation and potential source regions of $PM_{2.5}$-bound Pahs in the megacity Beijing, China: impact of regional transport. Environ Pollut 231:329–338

Zhou L, Chen XH, Tian X (2018) The impact of fine particulate matter ($PM_{2.5}$) on China's agricultural production from 2001 to 2010. J Clean Prod 178:133–141